

EXPERIMENTAL OBSERVATIONS OF IN-SITU SECONDARY ELECTRON YIELD REDUCTION IN THE PEP-II PARTICLE ACCELERATOR BEAM LINE^a

M. T. F. Pivi^b, G. Collet, F. King, R. E. Kirby, T. Markiewicz, T. O. Raubenheimer,

J. Seeman

SLAC, 2575 Sand Hill Road, Menlo Park, California 94025, USA

F. Le Pimpec

Paul Scherrer Institute, 5232 Villigen PSI, Schweiz

Abstract

Beam instability caused by the electron cloud has been observed in positron and proton storage rings and it is expected to be a limiting factor in the performance of the positron Damping Ring (DR) of future Linear Colliders (LC) such as ILC and CLIC [1, 2]. To test a series of promising possible electron cloud mitigation techniques as surface coatings and grooves, in the Positron Low Energy Ring (LER) of the PEP-II accelerator, we have installed several test vacuum chambers including i) a special chamber to monitor the variation of the secondary electron yield of technical surface materials and coatings under the effect of ion, electron and photon conditioning *in situ* in the beam line ii) chambers with grooves [3] in a straight magnetic-free section and iii) coated chambers in a dedicated newly installed 4-magnet chicane [4] to study mitigations in a magnetic field region. In this paper, we describe the ongoing R&D effort to mitigate the electron cloud

^a Work supported by the Director, Office of Science, High Energy Physics, U.S. DOE under Contract No. DE-AC02-76SF00515

^b Corresponding author: mpivi@slac.stanford.edu, +1 (650) 796 6986

effect for the LC damping ring, focusing on the first experimental area and on results of the reduction of the secondary electron yield due to *in situ* conditioning.

Keywords: Linear Colliders, Beam Instability, Electron Cloud, Secondary Electron Yield

1.0. Introduction

In accelerator beam lines with positively charged beams, an electron cloud may be initially generated by photoelectrons or ionization of residual gas and increase by the surface secondary emission process. If an electron cloud forms in the accelerator beam line, it may couple with the circulating beam and cause beam instabilities, tune shift, vacuum pressure rise, ultimately affecting the machine performances. The electron cloud has been observed at many storage rings and it will likely be an issue for future machines aiming at high beam intensity [1].

Over the last few years at SLAC, we have investigated several possible countermeasures to reduce the electron cloud effect in the LC DR and we invested considerable effort on both simulation and experimental programs. During the last years of running of the PEP-II collider, in the Region 12 straight section of the positron beam line just downstream of the arc section, we have installed vacuum chambers consisting of three experimental areas to test electron cloud mitigations both in field-free and magnet regions [3, 4]. In this paper, we describe a dedicated chamber installed to monitor the secondary electron emission coefficient or secondary electron yield (SEY or δ) of TiN and TiZrV non-evaporable getter (NEG) coating, Copper, Stainless Steel and Aluminum conditioning in the beam line *in situ* under the effect of electrons, photons and ions impacting the surface.

We have instrumented the chamber with a retarding field analyzer (RFA) [5, 6, 7, 8] electron detector to measure the intensity of the electron cloud current and the electron energy distribution. The RFA is described in a separate paragraph below. The goal of the experiment was to measure the change in the surface SEY and surface structure composition of sample materials directly exposed to dynamical beam effects and compare the results to the typical reduction of the SEY observed in laboratory set-ups when a material is irradiated with electron beams. Other suppression techniques such as clearing electrodes, grooves and novel coatings are also being tested and optimized at several other laboratories including CERN, INFN, in CesrTA at Cornell University, and KEK-B at KEK.

2.0. Secondary Electron Yield SEY

Parameters determining the cloud formation are the secondary electron yield, secondary electrons emitted per incident electron, and the secondary electron energy spectrum. Typically, the peak value (δ_{\max}) of the SEY, at normal incidence, is $\delta_{\max} \sim 1.5 \div 2.2$ for an “as-received” technical vacuum chamber material such as copper or stainless steel but ranges higher, for aluminum, at $\delta_{\max} \geq 2.3$ and can be over 3. The laboratory experimental set-up used at SLAC to measure the surface SEY and perform surface X-Ray Photon Spectroscopy is described in detail in the references [9, 10]. Note that in the apparatus, the SEY is measured with the use of an electron beam incoming at a 23° angle with respect to the sample surface normal. The SEY of technical surfaces material for accelerator vacuum chamber has been measured in the past at CERN [11, 12] at KEK [13, 14, 15] SLAC [9, 16, 17] and at other laboratories [18].

2.1. SEY Threshold and Requirements

Previous simulations show that in a 6 km ILC DR an electron cloud is expected to develop with high densities for peak SEY values above 1.2.

In the ILC DR, a threshold for beam instability [2] will be reached for a cloud density of $1.4 \cdot 10^{11} \text{ e/m}^3$. The most robust solution to mitigate the electron cloud is to ensure that the vacuum chamber wall has low secondary emission yield.

The impact of particles on a metallic surface reduces the surface SEY to low values [9-17]. This effect is known as conditioning. Typically, conditioning is provided by, electrons from the electron cloud or photons and ions generated by the circulating beam. Even following the surface conditioning, electron clouds are still observed at several existing storage rings as CernTA, Daphne and the B-factory KEKB. The efficiency of the conditioning may depend on several factors including the electron cloud current or radiation impinging the surface, the vacuum chamber material as well as the residual vacuum pressure. A competing effect to conditioning is the surface recontamination by the residual gas when the circulating beam is not present. Recontamination may increase the SEY over time. Thus, it is important to measure the effect of conditioning of samples exposed directly to an accelerator beam line as well as the recontamination effect.

3.0. Dedicated Vacuum Chamber Experimental Setup to Monitor the Reduction *in-situ* of the Secondary Electron Yield

To closely monitor the evolution of the SEY in an accelerator environment, we have built and installed a dedicated stainless steel in the PEP-II beam line. The chamber is

instrumented with manipulators and transferring systems to i) expose the samples to the beam environment then ii) transfer the samples to a laboratory set-up [9,10] and iii) measure their surface characteristics. It is crucial to maintain the samples in ultra-high vacuum (UHV) during transferring. This is achieved by means of specially designed load-lock manipulators provided with valves to insert samples in their working position and to retract them in a load-lock UHV chamber for transportation. Figure 1 shows the chamber installation in the PEP-II LER. The load-lock manipulator system used to position the sample into the beam line is shown in Figure 2.

The design of the vacuum chamber allowed the insertion of two samples at a time and at two different angles: i) directly exposed to the fan of synchrotron radiation and we will refer to as 0° angle or ii) at an angle 45° from the middle plane out of the synchrotron radiation fan.

During beam operation, the samples are left in the beam line for a period of several weeks until access to the machine tunnel is possible.

In particular during the installation in the beam line, the samples were positioned in contact with the chamber wall and facing the internal side of the beam line, as shown in Figure 3-Center.

The positioning of the samples in the PEP-II beam line had to be done precisely for two reasons: i) any misalignment of the sample would prevent the synchrotron radiation from the bend to hit its surface due to masking issue ii) to avoid the presence of spacing and cavities that would cause leakage of the beam radiofrequency into the load-lock system that in turn would cause overheating and ultimately melting of components. In both cases, an overheating or melting of components would have compromised the success of

the experiment. To align the sample precisely in position with its surface aligned to the chamber surface and with correct curvature orientation, the vacuum port on the chamber hosting the sample was welded with high precision tools. Also, the final section of the vacuum port was tapered down to drive the sample into its working position as shown in Figure 3-Center.

The sample housing and the spacing between the sample and the chamber wall had to be carefully designed to avoid both the trapping of higher order modes (HOM) propagating along the beam line and again leakage of radiofrequency from the beam into the manipulator itself. To absorb any leaking RF, the samples were designed with two circular cuts where we have arranged Copper-Beryllium “RF” springs.

Furthermore, synchrotron radiation generated by the beam passing by the last dipole magnet in the upstream arc amount to $P_{SR}=455$ W/mrad emitted per mrad of bend [19] in the horizontal plane according to the design beam parameters of Table 1. The sample located at a distance of 10.1 m from the last magnet and was irradiated by 3.5 W of power that needed to be removed. To remove the heat load from the sample, the RF springs have been silver plated to increase the mechanical contact and to allow a good thermal exchange between the sample and the chamber wall.

The stainless steel chamber was externally copper clad and a water cooling line was welded along the external body of the chamber, close to the horizontal middle plane at the level of the synchrotron radiation fan.

To monitor the temperature increase due to synchrotron radiation or HOM, several thermocouples were arranged at different locations on the external side of the chamber and at the vacuum port locations.

A detailed procedure had to be followed during each sample loading or removal into the PEP-II beam line.

The procedure to manually install the samples into position in the accelerator beam line is as follow. The sample is first secured inside the manipulator at the end of an arm magnetically coupled with a linear pushing device. Vacuum is made inside the manipulator. Thus, the manipulator is connected to the vacuum chamber in the beam line. Two valves secure the vacuum pressure. Once the manipulator is connected to the vacuum chamber, the valves are open after having evacuated the gap between the valves. The manipulator arm is then manually extended, passed the valves to position the sample in the beam line. Once the sample is aligned with the chamber surface, the accelerator operations can resume. The sample is left in the beam line for several weeks of conditioning and until access at the machine is stopped. During a machine stop and when the machine tunnel is accessible, the sample is retracted until visible by a window located on the manipulator, the valves are closed and the manipulator is disconnected from the beam line. The manipulator is then transported and connected to the laboratory measurement set-up [10]. The sample is manually and mechanically transferred into the analysis chamber under high vacuum to avoid contamination from air. Contamination from water and oxides modifies the composition of the first few mono-layers and re-increase the surface secondary electron yield, thence removing the beneficial effect of conditioning [10,11].

The manipulator is provided with a port connected to valves and an ion pump to ensure high vacuum. The vacuum pressure was typically $1 \cdot 10^{-7}$ Torr during sample transportation and transferring.

3.1. Electron Cloud Monitor and Retarding Field Analyzer (RFA)

An electron cloud monitor was installed in the middle of the chamber between the two load-lock systems as shown in Figure 1. The design of the electron monitor is shown in Figure 4. The monitor had a twofold functionality: to collect the electron cloud current and to measure the electron energy by the retarding field analyzer method. The analyzer consisted of 4 grids and an electron collector located behind the grids. When used in electron current detection mode, the 4 grids were typically grounded, while when used in energy analyzer mode, the inner most grid and the external most grid were grounded while the 2 central grids were biased with a negative potential varying between 0 V and -500 V. A negative grid potential prevents the electrons from reaching the collector, thus selecting the electrons in energy. The electron cloud distribution is then obtained by differentiation of the integrated collector electron current.

The RFA was designed with 4 grids to ensure uniform electric field lines.

The holes in the vacuum chamber for the electron cloud current detection had to be carefully designed to avoid penetration of the beam RF into the detector cavity. To minimize the propagation of the beam RF into the detector housing, the holes were chosen to have a diameter $\phi = 1$ mm for a chamber wall thickness of 3 mm, thus with a hole depth:diameter ratio of 3:1, see Figure 5. The total area of the holes was ~18% and it was chosen during the design to minimize the impact on the electron cloud development

but to maximize the collection of electron current. The cumulative area of the holes was 1.3 cm². The electron current is normalized to this value to obtain the electron flux in units of A/cm².

4.0. Photon, Electron and Ion Doses on the Samples

The beam current in the Positron PEP-II Low Energy Ring during the installation of the TiN samples in the beam line is show in Figure 6. The measured electron cloud current as a function of the positron beam current is shown in Figure 7.

4.0.1. Photon dose

In general one may assume that each positron generates on average N_{γ/e^+} incoherent photons of all energies and directions emitted by each positron traversing each dipole magnet

$$N_{\gamma/e^+} = \frac{5\alpha\gamma}{2\sqrt{3}} \Delta\theta \quad (1)$$

where γ is the relativistic factor and $\alpha=1/137$ is the fine structure constant and $\Delta\theta$ is the dipole magnet arc section in degree. As an example, each positron on average emits $N_{\gamma/e^+} = 2.09$ photons at any energy and angle upon traversing the upstream dipole magnet [20], with beam parameters shown in Table 1. Eq. (1) represents the total number of photons emitted by a beam particle while traversing a dipole. To estimate the photon dose on the sample, we need to calculate the number of photons hitting the sample and thus integrate the spectrum of synchrotron radiation [21],

$$\frac{dN_{\gamma/e^+}}{dn d\phi d\psi} = \frac{\alpha}{3\pi^2} n(\gamma^{-2} + \psi^2)^2 \left[K_{2/3}^2(\xi) + \frac{\psi^2}{\gamma^{-2} + \psi^2} K_{1/3}^2(\xi) \right] \quad (2)$$

where this formula represents the number of photons radiated into a fan out-of-plane opening angle $d\psi$ when a positron moves at constant speed ω_0 with relativistic factor $\gamma \gg 1$ through an arc of circle $d\phi$. The $K_n(\xi)$ are modified Bessel functions, and n is the harmonic number of the radiation $n = \omega/\omega_0 = E/h\nu_0$ where E is the photon energy. The parameter ξ is defined by $\xi = \frac{n}{3}(\gamma^{-2} + \psi^2)^{3/2}$. The estimation of N_{γ/e^+} is done by numerical integration over the proper dipole arc section along which the generated photons will continue their path and hit the sample. After integration of eq. (2) one obtains N_{γ/e^+} the number of photons per positron emitted in an opening angle $1/\gamma$, we compute the photon dose D_{ph} over time by

$$D_{ph} = \int_{t_1}^{t_2} \frac{I(t)N_{\gamma/e^+}}{e} dt \quad (3)$$

where e is the positron charge and the beam current varies with time $I = I(t)$, as shown for example in Figure 6. Eq. (3) represents the number of direct photons hitting a sample during the exposure time interval $(t_2 - t_1)$. We will express the dose in [photon/mm²] after normalizing by the effective radiated sample area = 28 mm². In estimating the dose, we do take into account direct radiation from the two upstream dipole magnets and we do not take into account multiple reflections inside the vacuum chamber. The calculated photon dose for the samples located on the horizontal plane is shown on Table 2. In the case of the samples located at a 45 degree out of synchrotron radiation fan, the number of direct photons that hit the sample surface is negligible. Nevertheless, a considerable number of photons are reflected multiple times and strike the vacuum chamber at any

azimuth position and thus photon conditioning still take place for samples located at 45 degree angle.

4.0.2. Electron dose

We estimated the electron dose defined as the number of electrons in the cloud that impinge into the vacuum chamber surface. The electron current is measured by the electron detector. The electron dose in units [mC/mm²] is calculated by integrating the flux of electrons at the electron collector

$$D_e = \int_{t_1}^{t_2} F(I(t))dt \quad (4)$$

where the measured electron flux $F = F(I)$ is a function of the positron beam current I , as shown in Figure 7, and the beam current varies with time $I = I(t)$, as shown for example in Figure 6. Finally, the integration limits t_1 and t_2 are the initial and final time in the beam line, as shown in column 7 in Table 2.

4.0.3. Ion dose

To estimate the effect of ion conditioning, we assume that the positron beam circulating in the experimental chamber, of 89 mm diameter, see Table 1, has a Gaussian profile. The largest energy kick to the ion will be generated by a beam with smallest transverse dimensions. The energy of the ions when reaching the chamber wall, assuming a 1 r.m.s. transverse beam size is given in Table 3. When assuming 3 r.m.s beam sizes, the ions energy gain is converging to about 250eV. In those energy ranges, the ions are very effective at sputtering the surface [17, 22]. The cumulative charge of ions necessary to reduce the SEY max of TiN or NEG films, to a value obtained after electron conditioning is a factor 2000 lower [17]. The ion dose is calculated according to the PEP II beam

parameters, Table 1. The ionization cross section for a beam particle of energy above 100 keV can be calculated [23] by

$$\sigma = 4\pi Z^2 \left(\frac{\hbar}{mc} \right)^2 \frac{1}{\beta^2} (xM^2 + C) \quad (5)$$

where β is the relativistic coefficient, c the speed of light, m the electron mass, Z the charge, \hbar the Planck constant, M and C are constants depending on the molecules, and the function $x = 2 \ln(\gamma) - \beta^2$ for $\beta \sim 1$. At a positron beam energy of 3.1 GeV the cross section for CO^+ is ~ 1 Mbarn. The number of ions created is $N_{ions} = I_e \sigma N_{molec} L$, where L is the length of the vacuum chamber, N_{molec} is the number of molecules per unit volume and I_e is the positron beam current. Assuming an operating vacuum pressure of 10^{-9} Torr, the density of molecules $N_{molec} = 3.21 \cdot 10^7$ molecules/cm³. Each sample has seen different average beam current when installed in the beam line, as shown in Table 4.

For the highest beam current, the number of ions per second and per meter length of chamber is $N_{ions} = 0.36 \cdot 10^9$ ions/s/m. Thus, the ion impinging the wall is $1.3 \cdot 10^3$ ion/s/mm², over 1000 hours this corresponds to an accumulated dose of $D_{ions} = 0.74$ nC/mm². This ion dose has a negligible effect on lowering the surface secondary electron yield and conditioning [17].

5.0. Surface Analysis of Samples Exposed to Conditioning in the beam Line and Recontamination by Residual Gases

During the years 2007 and 2008, we have manufactured numerous samples with different materials including: copper, stainless steel and bare aluminum. A number of aluminum samples were also coated with thin films of TiN or TiZrV non-evaporable getter (NEG).

Below, we describe the procedure for the installation and measurements of the different sample materials. Aluminum samples were coated by a thin film coating of TiN with a typical thickness of 100 nm. As shown in Figure 8, the SEY of the two as received TiN/Al samples was $\delta_{\max}=1.71$ and 1.77 as measured before the samples installation in the beam line. Thus, the two samples were installed in the beam line at two different angles with respect to the synchrotron radiation fan. Following two months conditioning period and an electron dose of $\sim 900 \text{ mC/mm}^2$, the SEY decreased similarly in both samples down to $\delta_{\max}=0.92$ and 0.95 .

Note that an electron dose of $\sim 1 \text{ mC/mm}^2$ is sufficient to considerably decrease the SEY on most surfaces in a laboratory set-up system [24].

To quantify the elemental content on the samples surface, we performed surface analysis by X-Ray photon spectroscopy in the same laboratory system setup used to measure the SEY. Thus, the samples were kept at the same location for both analysis and without exposing them to external contamination. By surface analysis we found that Carbon and Oxygen contents were strongly reduced after conditioning of the TiN samples, Figure 9 and Figure 10 and Table 5. Our hypothesis is that carbon oxides and oxides may have been removed by a combination of photons, ions or electrons impinging with sufficient energy on the surface. This reduction in the carbon content is contrary to what is expected when only electrons impinge on a surface. In fact, electron beams impinging on a surface typically results in an increase of the carbon content as reported at various laboratories [10,22].

Following the conditioning period in the beam line, the TiN sample was kept in stand by in the laboratory set-up for 2928 hours or 122 days in ultra-high vacuum $< 10^{-9}$ Torr, and

in an atmosphere 10:1 of H₂:CO, typical of accelerator beam lines. Notably, the SEY of the TiN sample was still measured to be lower than 1, as shown in Figure 11. A secondary yield below unity considerably mitigates the formation of electron clouds in particle accelerators. The two TiN samples arranged at different positions with respect to the fan of synchrotron radiation showed a similar reduction in the SEY after conditioning, see Table 2, and similar carbon and oxygen depletion in the atomic surface content.

Figure 12 shows SEY results obtained with coated samples of TiZrV thin film NEG. The NEG coating was performed by S.A.E.S. Getter with a thickness of 1 μm . Thin films of NEG material have the peculiar feature to act as vacuum pumps if they are heated to high temperature for sufficient period of time. The process of heating the NEG until it starts acting as vacuum pump is also known as activation process [25]. A beneficial effect of the NEG activation is that surface oxides on the first few mono-layers are dissolved and absorbed into the bulk of the material and as a consequence the secondary electron yield decreases [11,16]. Aiming at the NEG activation, we have built a separate vacuum chamber with a heating system mechanism to allow pre-heating the NEG before installation in the beam line. Following the recipe suggested in the literature [26], we have heated the NEG sample at 200°C for more than 2 hours in the set-up. The activation chamber was made of stainless steel. Ideally, the activation chamber should have been entirely coated with NEG, to reduce the contamination on the NEG sample from outgassing. After heating, we transferred the sample in the surface analysis set-up and measured a SEY $\delta_{\text{max}} \sim 1.33$. The TiZrV sample is then installed in the PEP-II beam line and is exposed to the beam environment for several weeks. The sample was then

transferred back to the analysis set-up and measured with a SEY ~ 1.05 , as shown in Figure 12.

Furthermore, we have manufactured several samples in bare Aluminum 6063, Stainless Steel and Oxygen-Free Electronic (OFE) Copper and installed those in the beam line at different times. A summary of the SEY measurement results is shown in Table 2.

Following the beam line conditioning of an aluminum sample, the SEY reduced from an initial value of $\delta_{\max} \sim 3.3$ to a value after conditioning of $\delta_{\max} \sim 2.4$, Figure 13. This is unacceptably high to be used in LC DR and it is a concern for the development of an electron cloud in existing circular accelerators using aluminum vacuum chambers, as DAPHNE at LNF (Frascati National Laboratory) and CEsrTA at Cornell University. The finding about a high SEY for conditioned aluminum in the accelerator beam pipe is in good agreement with previous measurements of aluminum samples exposed to electron conditioning obtained in our laboratory system set-ups [10]. Surface analysis by X-Ray Photon Spectroscopy of the bare 6063 Aluminum sample as measured before and after exposition to the beam environment in the PEP-II beam line is shown in Figure 14 and the concentration of different elements in Table 6. Oxygen content is reduced, but Mg, which is present in Al 6063 alloy, is revealed as we have seen during electron conditioning [10]. The presence of the peak at 308 eV is a characteristic of oxidized Magnesium. Fluorine does not disappear and Nitrogen appears and shows a strong peak. Carbon almost completely disappears from the spectrum. These behaviors differ somewhat from what we have observed on the same Al alloy during a sole electron conditioning [10].

Electrons and photons are not able to remove the oxides on the aluminum surface and the ion dose is too low to have any effect. The result is that the oxide is not broken, but modified resulting in still a high SEY (>2). One should note that a sputter clean Aluminum surface has a SEY below unity [27].

A stainless steel sample was extracted from the beam line several hours after the stop of the positron beam. It was transferred into the surface analysis chamber and the SEY measured after 550 hour from the beam stop. PEP II priority is to produce beam for the BaBar detector, hence the long waiting period before accessing the sample. After extraction, we monitored the SEY during a couple of month of standing-by in the analysis chamber. Figure 15 shows the effect of stainless steel surface recontamination after ~ 8 weeks in ultra-high vacuum at $5 \div 10 \cdot 10^{-10}$ Torr. The SEY peak increased from $\delta_{\max} \sim 1.3$ to a value $\delta_{\max} \sim 1.6$ in about 1300 hours.

Finally, we have measured the electron energy distribution with the retarding field analyzer. The energy spectrum is obtained by scanning with a negative voltage the two central analyzer grids between 0V and -500V in steps of 1-2 eV during a period of time in which the positron beam current is maintained constant in the accelerator. The bias voltage V is assumed to repel the electrons with energy lower than $e \cdot V$. Then, the electron current I_e is measured at each Voltage step and represent the integral of all electron energies above the step voltage. The electron energy distribution is obtained by differentiation of the current signal over the energy, dI_e/dE , as shown in Figure 16. The two curves correspond to two different positron beam current respectively 2500 mA and 1500 mA. For both curves, the energy spectrum is peaked at low energies ~ 5 eV.

Finally, we would like to mention that microwave dispersion measurements [28] estimated an average electron cloud density of $6.6E+11 \text{ e/m}^3$ in a 50m PEP-II straight section located just downstream of our experimental chamber. This estimation of the cloud density should be considered as a lowest limit value for the cloud density in our experimental chamber upstream, due to its proximity to the bend and thus subjected to a higher rate of photoelectrons.

6.0. Summary

Several chambers were installed in the PEP-II LER to study the electron cloud effect and monitor the details of the secondary electron yield in a positron accelerator beam line.

We measured a drastic reduction of the secondary electron yield of TiN surfaces conditioned in the beam line to a value $\delta_{\max} \sim 0.95$. The secondary electron yield persisted below 1 even following thousand hours of standing-by in a vacuum environment without beam. XPS analysis shows a drastic reduction of the C1s and O1s peak, suggesting the removal the oxides. For the aluminum surface we measured a secondary electron yield exceeding 2, even after conditioning for several months in the positron beam line, making bare aluminum an unacceptable surface for the Linear Collider applications when electron multiplication is expected. The positron beam does not produce enough ions to condition the surface. Electron and photon bombardment, created by PEP II, are not sufficient to break the natural aluminum oxides responsible for a high SEY.

Several other technical vacuum chamber materials were measured including non-evaporable getter thin film coated surfaces.

TiN thin film coating has been demonstrated to have an SEY below the instability threshold for the Linear Collider Positron Damping Ring and as today should be regarded as a candidate coating material in the accelerator sections where the electron cloud is expected the most. Work continues to address remaining issues such as coating durability. Yet, requirements at future colliders are very stringent, such as an unprecedented geometric vertical emittance of 2 pm in the ILC DR or sub-pm emittance for the CLIC DR. Hence, a close collaboration between laboratories is underway to develop other mitigation techniques that are complementary to coating, to further suppress the electron cloud effect down to comfortable levels. A draft of the recommendation for electron cloud mitigations in the LC DR is also presented in Table 7, to be completed as input for LC Technical Design Phase.

All the PEP-II experimental chambers, instrumentation and diagnostics have now being re-deployed into the CESR-TA [29] test facility at Cornell University, to continue the studies in the framework of the LC international collaboration.

ACKNOWLEDGMENTS

The authors wish to thank D. Kharakh for all the installation, D. Blankenship, D. Arnett and N. Kurita for the critical design phase, F. Cooper, M. Munro for great help during, construction and installation, H. Imfeld for the chambers alignment, L. Wang, N. Phinney, J. Ng for very useful discussions, the Vacuum department and the PEP-II operation group for great support during the projects commissioning and testing. Also, we would like to thank the fruitful LC international collaboration that is leading to a successful R&D program on electron cloud mitigations.

LIST OF TABLE

Table 1. Nominal beam parameters in the PEP-II Positron Low Energy Ring.

Beam Energy, E (GeV)	3.1
Relativistic Factor, γ	6066.5
Nominal Beam Current, I (A)	4.7
Dipole Magnet Field, B (Tesla)	0.765
Critical Energy, E_{crit} (keV)	4.8
Dipole Magnet Arc Section, $\Delta\theta$ (mrad)	32.7
Dipole Arc Section of photons hitting sample, $\Delta\theta$ (mrad)	$7.5 \cdot 10^{-6}$
Distance of last bend magnet to SEY station location, (m)	10.1
Bunch length (mm)	12
Spacing between bunches (ns)	4.2
Transverse beam size at the sample (x/y) (μm)	228/840

Table 2. Summary of the measurements taken on the samples installed in the PEP-II beam line. SEY before installation and after conditioning in the beam line. The sample position is specified with respect to the synchrotron radiation (SR) fan located in the horizontal middle plane. The two possible sample positions were at 0° or 45° respectively “in” or “out” of the synchrotron radiation fan. The electron dose is computed at the electron analyzer located in the middle of the chamber between the two sample locations. The photon dose is computed using eq. (2) and (3).

	Peak SEY before	Peak SEY after	Sample position respect to SR	Electron dose D_e [mC/mm ²]	Photon dose D_{ph} [ph/mm ²]	Time frame in the PEP-II beam line	Equivalent Integrated beam current [A·hour]	Additional Notes
TiN/Al	1.77	0.95	in fan	910	$8.45\text{E}+20$	22Dec06	2198	Still SEY < 1

						to 26Mar07		after 1000h stand-by in vacuum
TiN/Al	1.71	0.92	out of fan	910	---	22Dec06 to 26Mar07	2198	SEY < 1 after 1000h stand-by in vacuum
NEG TiZrV/Al	1.33*	1.09	In fan	1183	1.06E+21	04Dec07 to 27Feb08	2767	*sample was heated before installation
Cu	1.8	1.22	in fan	902	6.92E+20	27Feb08 to 08Apr08	1799	
Stainless steel	1.85	1.3*	out of fan	1667.5	---	15Jun07 to 24Sep07	3388	*measured 500h after beam stop
Al	3.5	2.4	out of fan	2085	---	24Sep07 to 08Apr08	4566	

Table 3. Energy gained by ions when accelerated by the passage of successive positron bunches.

e ⁺ beam current	Horizontal kinetic E (eV)		Vertical kinetic E (eV)	
	H ₂	CO	H ₂	CO
1.81 A	589	473	357	356
1.25 A	400	390	293	293

Table 4. Average beam current and total beam time in hours, for each sample installed in the beam line.

	Average beam current [A]	Total number of beam operating hours
TiN/Al	1.25	1758
NEG TiZrV/Al	1.52	1820
Cu	1.81	993
Stainless Steel	1.74	1947
Al	1.62	2818

Table 5. TiN surface composition, by X-Ray Photon Spectroscopy, before and after beam conditioning in the PEP-II beam line. Note the relative decrease of the Oxygen and Carbon content with respect to the other elements.

Elements in the XPS spectrum	Concentration before beam exposure (at%)	Concentration after beam exposure (at%)
O	29.7	21.50
Ti	22.32	36.52
N	35.93	37.81
C	21.98	3.63
Cl	none	0.42

Table 6. Al 6063 surface composition, by X-Ray Photon Spectroscopy, before and after positron beam exposure in the PEP-II beam pipe. Note the relative content of Oxygen, revealing that oxides are still present after exposition to the beam line. Mg and N are present after exposition.

Elements in the XPS spectrum	Concentration before beam exposure (at%)	Concentration after beam exposure (at%)
Mg	0.6	11.3
F	1.9	1.7
O	53.6	40.5
N	-	9.6
C	13.3	2.8
Al	30.6	34.1

Table 7. Draft of the recommendation for electron cloud mitigations. This table is to be completed as input for ILC Technical Design Phase. The table has been discussed by the ILC community during the ILC DR Workshop at Albuquerque, New Mexico, held in September 2009 and it is currently under evaluation. Amorphous-Carbon coating is being tested at CERN and CesrTa.

DR element	% Ring	Need For Antechamber	Coating	Mitigation	Additional if necessary
DRIFT in STRAIGHTs	54	No	NEG or amorphous-C	Solenoid	Grooves
DRIFT in ARCs	33	downstream of BEND only	NEG	Solenoid	Grooves
BEND	7	Yes	TiN	Grooves	
WIGGLER	3	Yes	TiN	Clearing Electrodes	
QUADRUPOLE	3	downstream of BEND / WIGG	TiN	Grooves	

LIST OF FIGURES

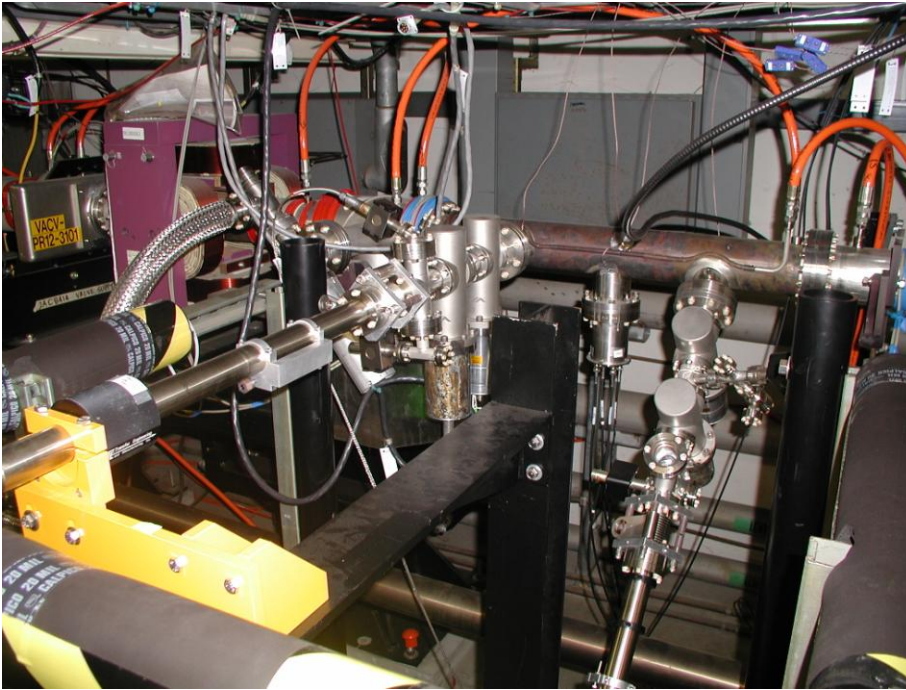


Figure 1. Installation of the SEY test chamber in the PEP-II LER beam line, the chamber and the two sample transferring load-lock manipulator systems are visible at 0° and 45° positions. The electron detector and energy analyzer is also visible on the chamber located between the two manipulators.

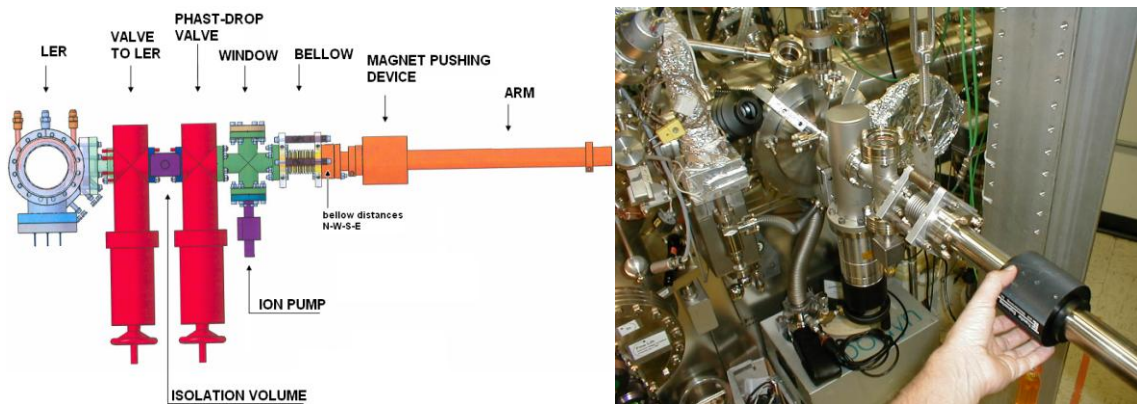


Figure 2. Layout (Left) of the load-lock system for positioning and transportation of samples under high vacuum. Load-lock system (Right) attached to the surface analysis chamber for transferring samples under vacuum.

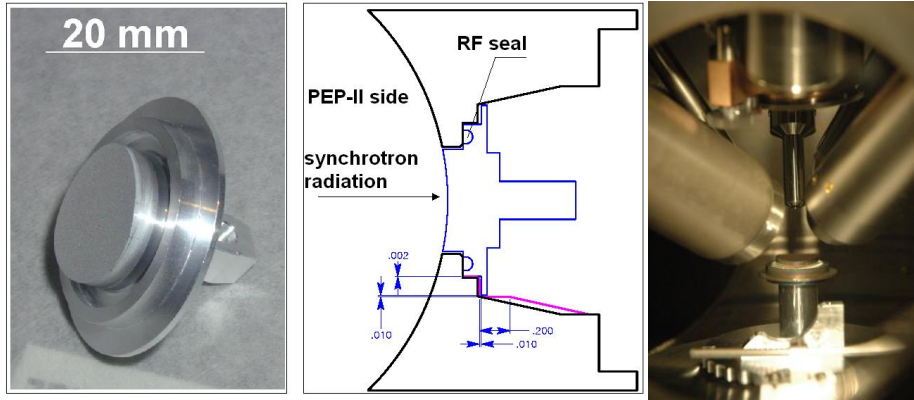


Figure 3. Left-Center-Right respectively: aluminum sample, layout of the sample installed in the PEP-II LER chamber and sample positioned in SLAC laboratory set-up for surface analysis. The sample surface exposed into the chamber and to synchrotron radiation has a diameter of 17 mm.

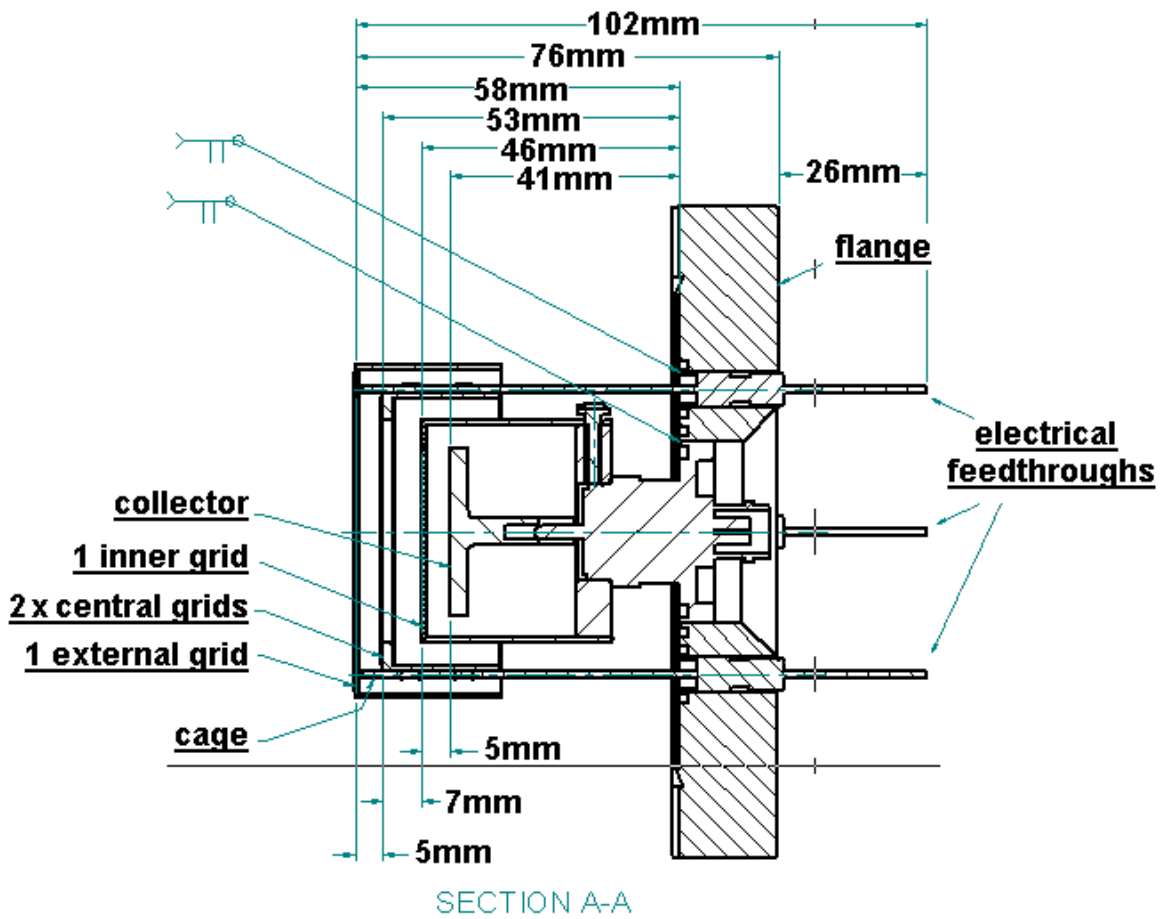


Figure 4. Layout of the electron detector and retarding field analyzer RFA consisting of 4 grids and a collector. When used in electron current detection mode,

the 4 grids are typically grounded, while when used in energy distribution mode, the 1 inner most grid and the 1 external most grid are grounded while the 2 central grids are biased with a potential scanned between 0V and -500V. The energy spectrum is obtained by differentiating the collected integrated electron current.

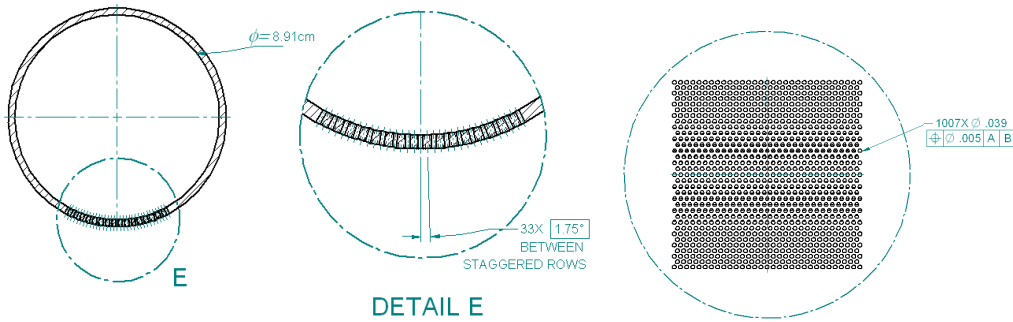


Figure 5. Schematic of the holes in the PEP-II chamber for the electron detection. The axis of the holes is radial with respect to the center chamber.

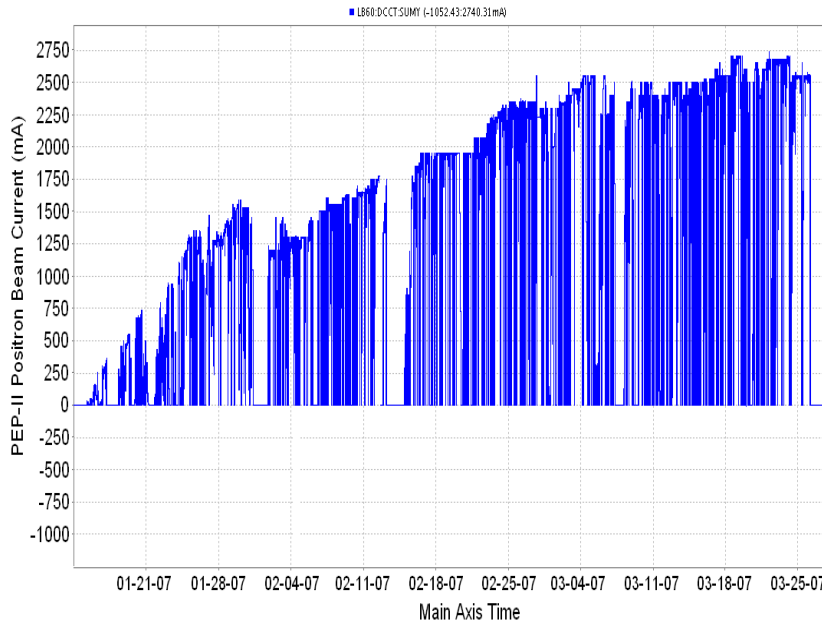


Figure 6. Beam current in the Positron PEP-II Low Energy Ring during the installation of the TiN samples in the beam line.

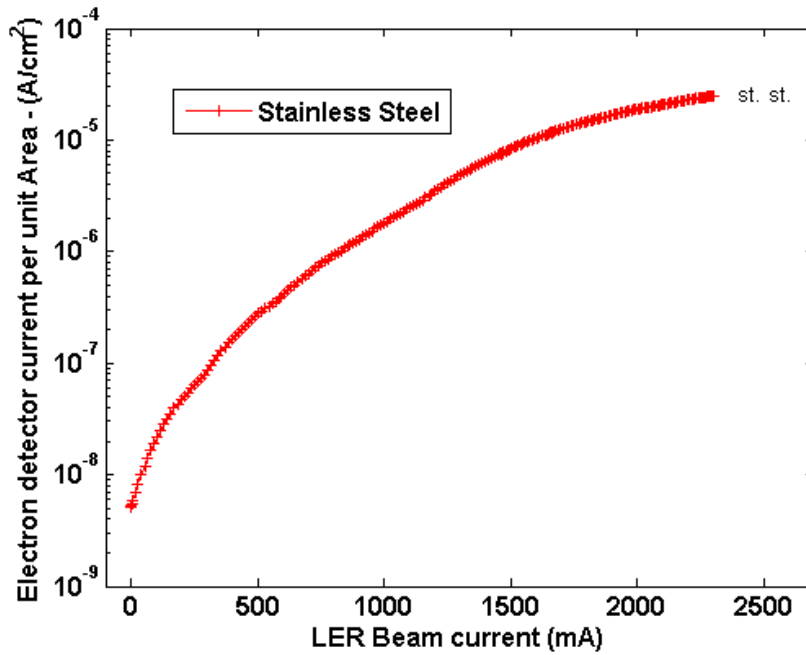


Figure 7. Experimental observation of the collected electron cloud signal [A/cm²] in the stainless steel chamber as a function of the PEP-II positron beam current. The electron signal at 0mA beam current represents the pedestal in the detector measurements.

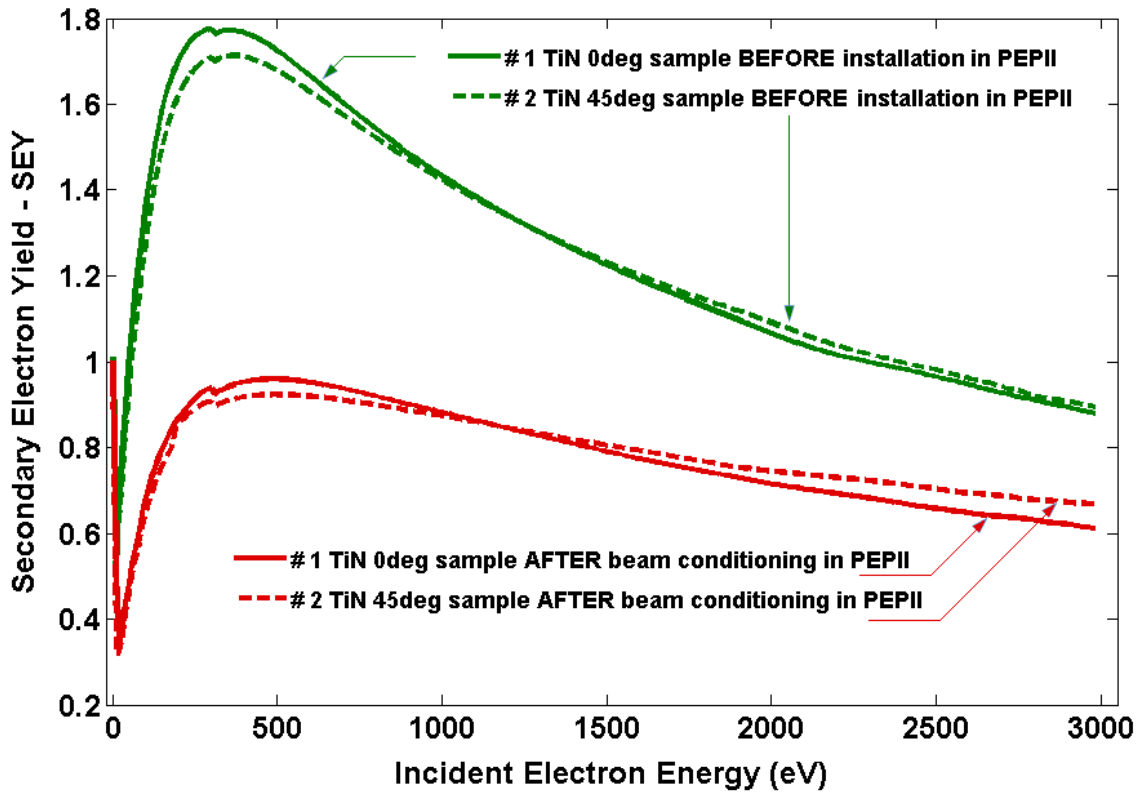


Figure 8. Secondary Electron Yield as measured before and after conditioning in the PEP-II beam line. The two TiN/Al samples were inserted in the PEP-II stainless steel chamber respectively in the plane of the synchrotron radiation fan (0° position) and out of this plane (45° position).

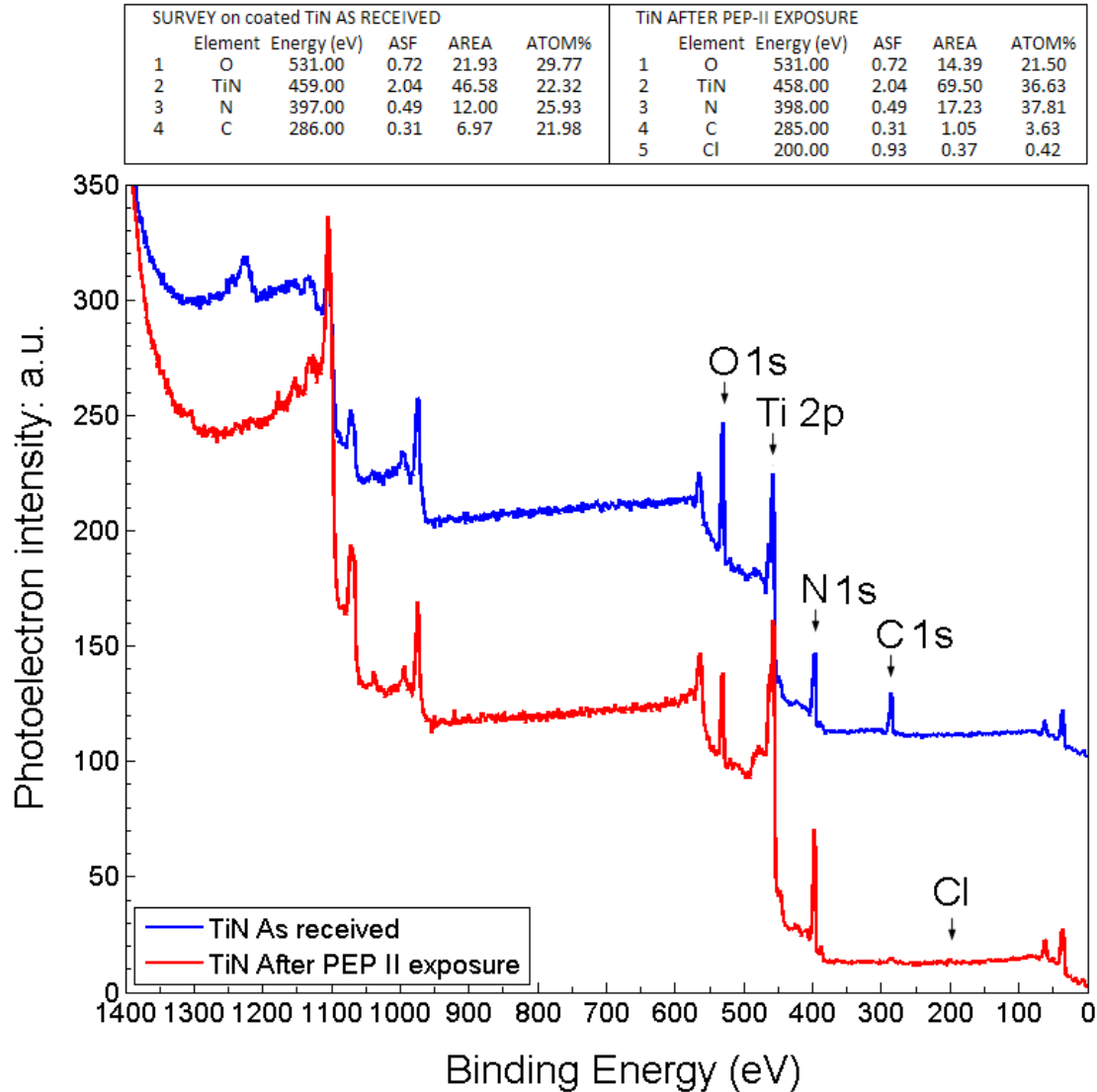


Figure 9. Surface X-Ray Photon Spectroscopy of the TiN sample as measured before (blue curve) and after (red curve) conditioning in the PEP-II beam line, related to Figure 8 and Figure 11. Carbon and Oxygen contents are reduced after exposition to the beam environment. This analysis is similar for the two TiN samples positioned at the two different locations in the test chamber.

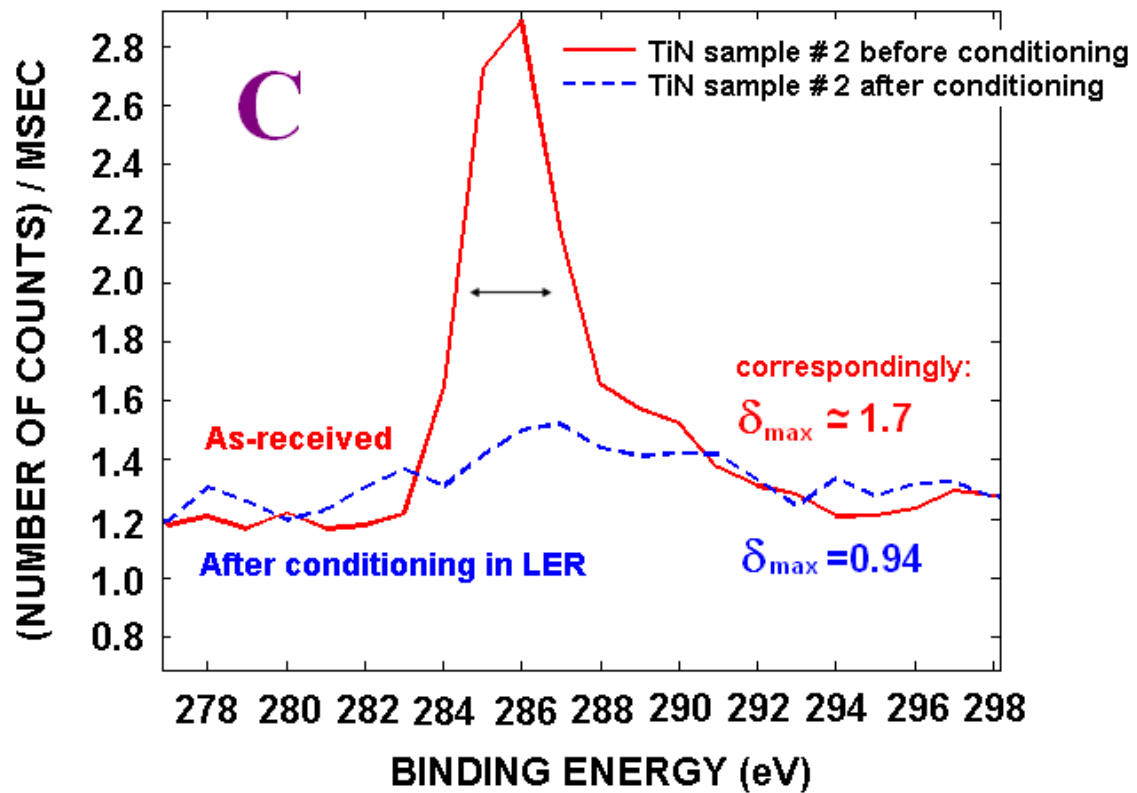


Figure 10. Details of the previous Figure at the C peak for the TiN sample. The corresponding SEY values for the sample before and after conditioning are also shown.

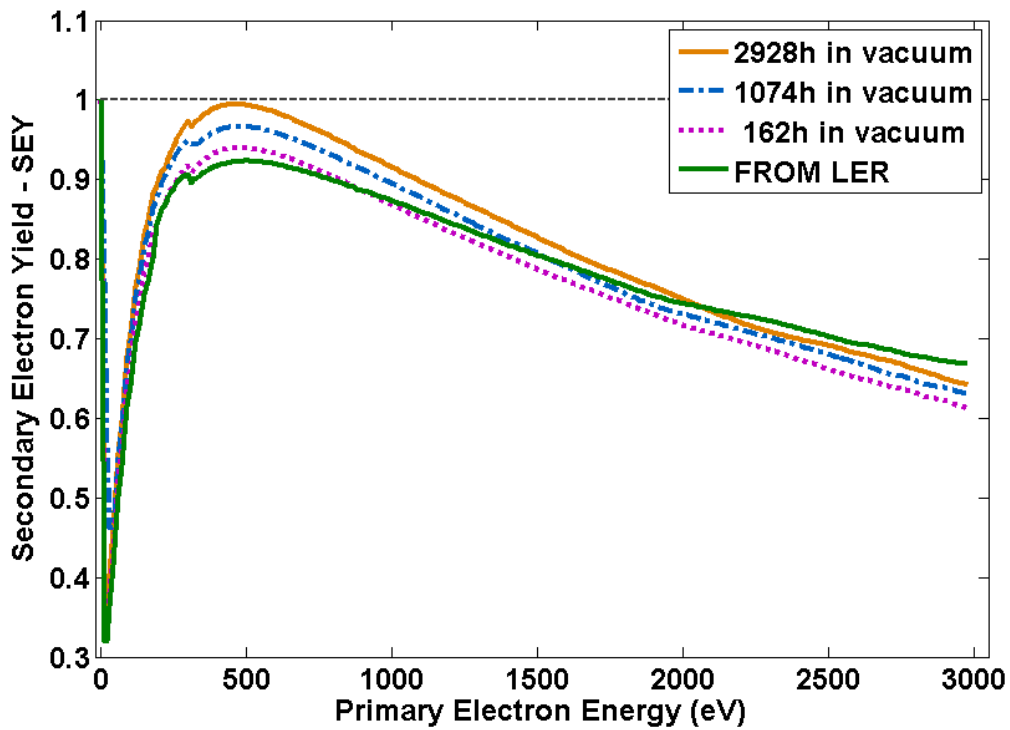


Figure 11. Effect of re-contamination of the TiN sample left in stand-by for over 2900 hours (122 days) in the analysis chamber following the conditioning period in PEP-II LER. The SEY seems stably below $SEY < 1$. In a vacuum pressure typical of an accelerator environment: $< 10^{-9}$ Torr, 10:1 H₂:CO.

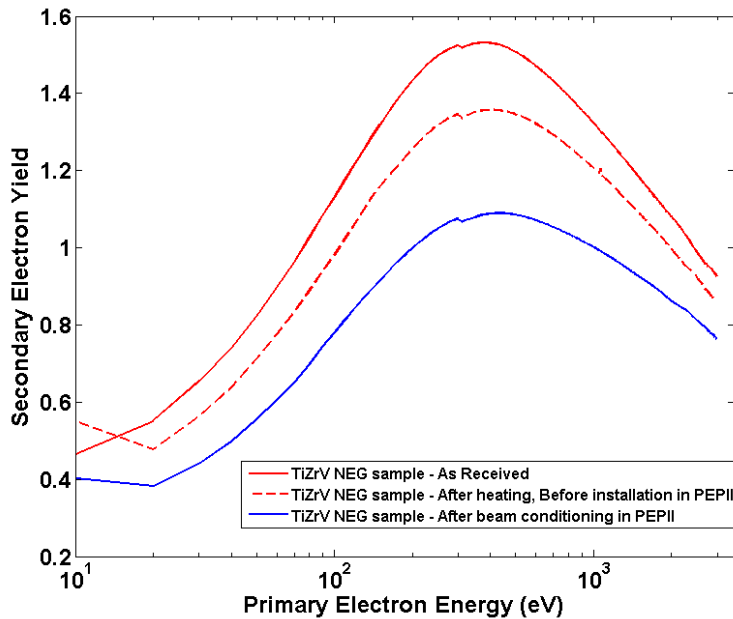


Figure 12. TiZrV Non-evaporable getter as received, following heating up of the sample at 200degC for 2 hours and after conditioning in the beam line.

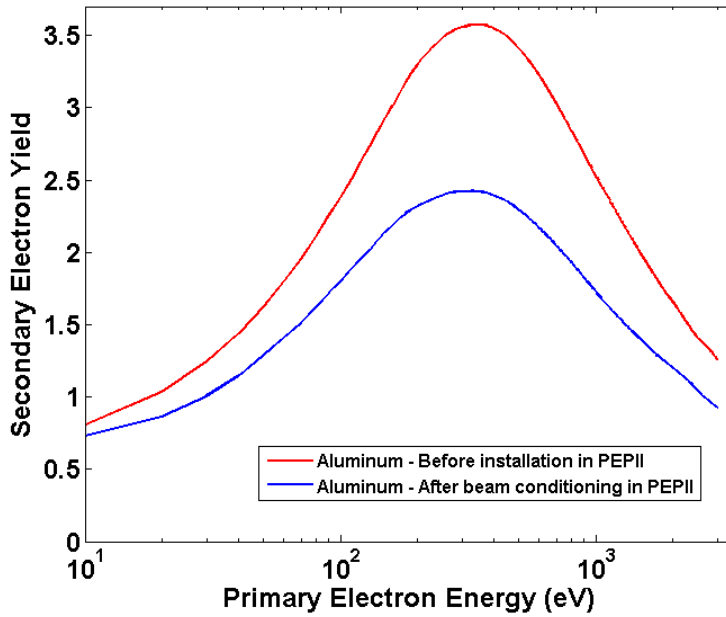


Figure 13. SEY of aluminum remains high with $\delta_{max} > 2$ even after more than 4500 A-hour conditioning in the beam line.

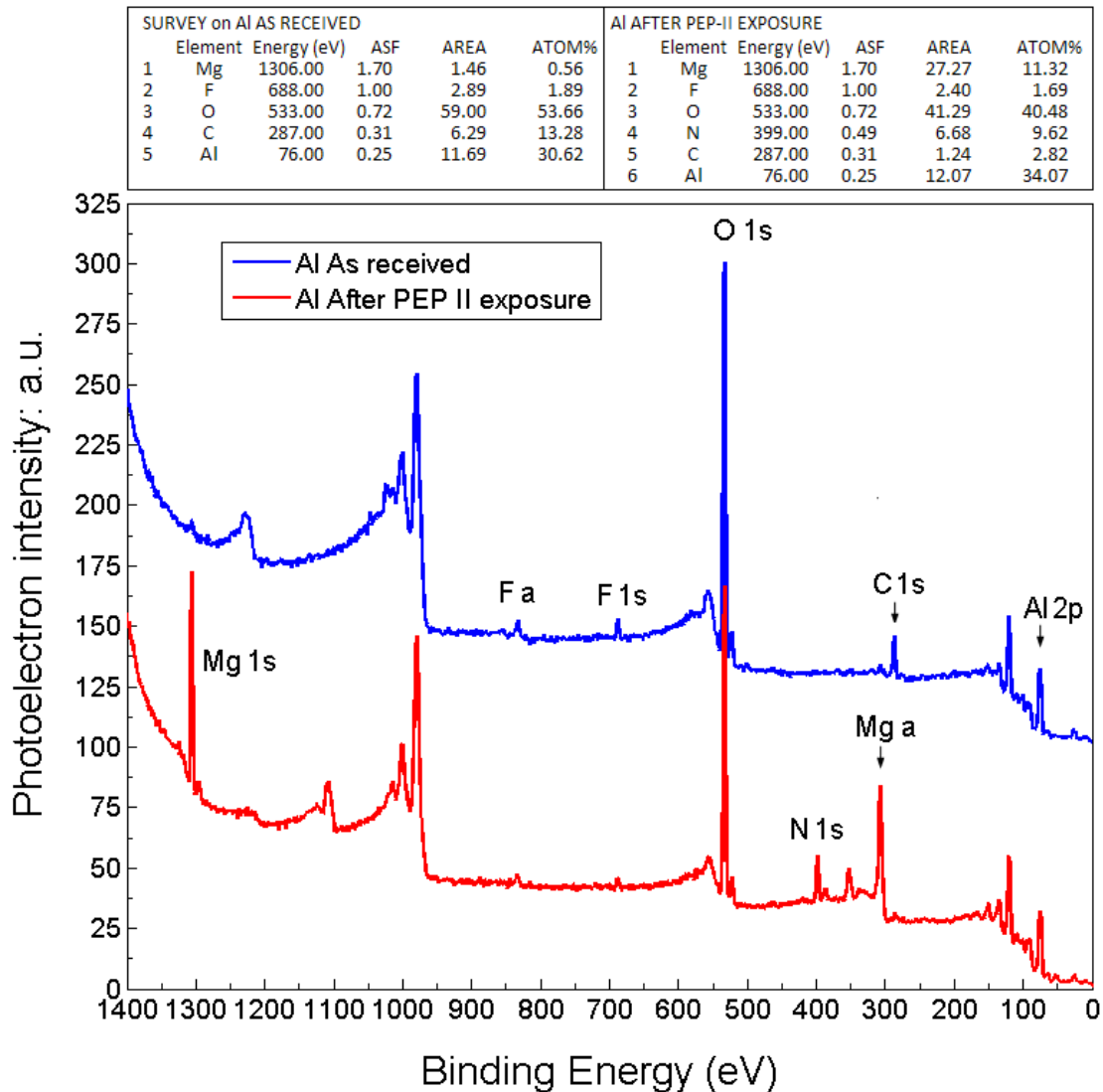


Figure 14. Surface X-Ray Photon Spectroscopy of the bare Aluminum sample as measured before (blue curve) and after (red curve) conditioning in the PEP-II beam line. Carbon content is reduced after exposition to the beam environment. Instead, Oxygen content was not reduced. Photons were not able to remove the oxides and there are not enough ions resulting in a clean aluminum oxidized surface with a high secondary electron yield, as shown in Figure 13.

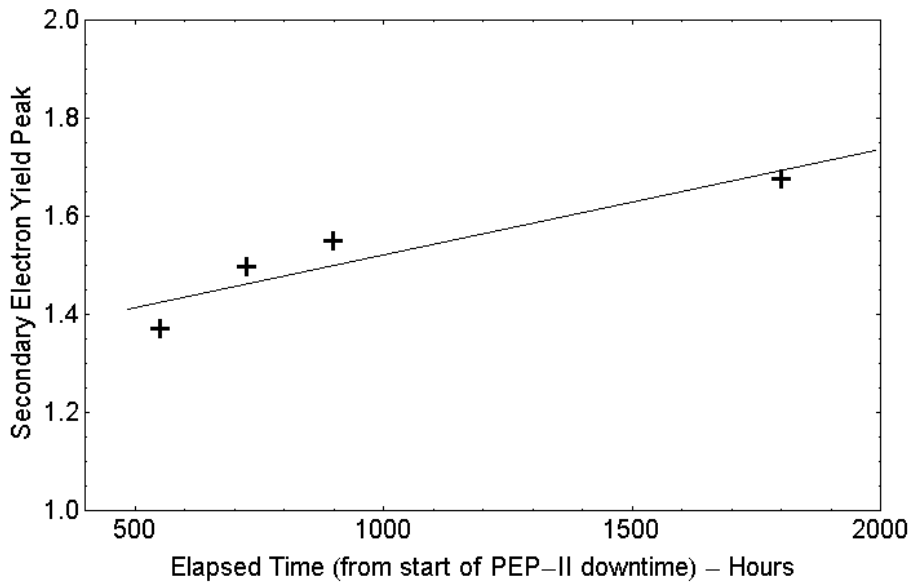


Figure 15. Yield vs re-contamination time for a stainless steel sample left in stand-by in high vacuum in the analysis chamber, following the conditioning in the beam line.

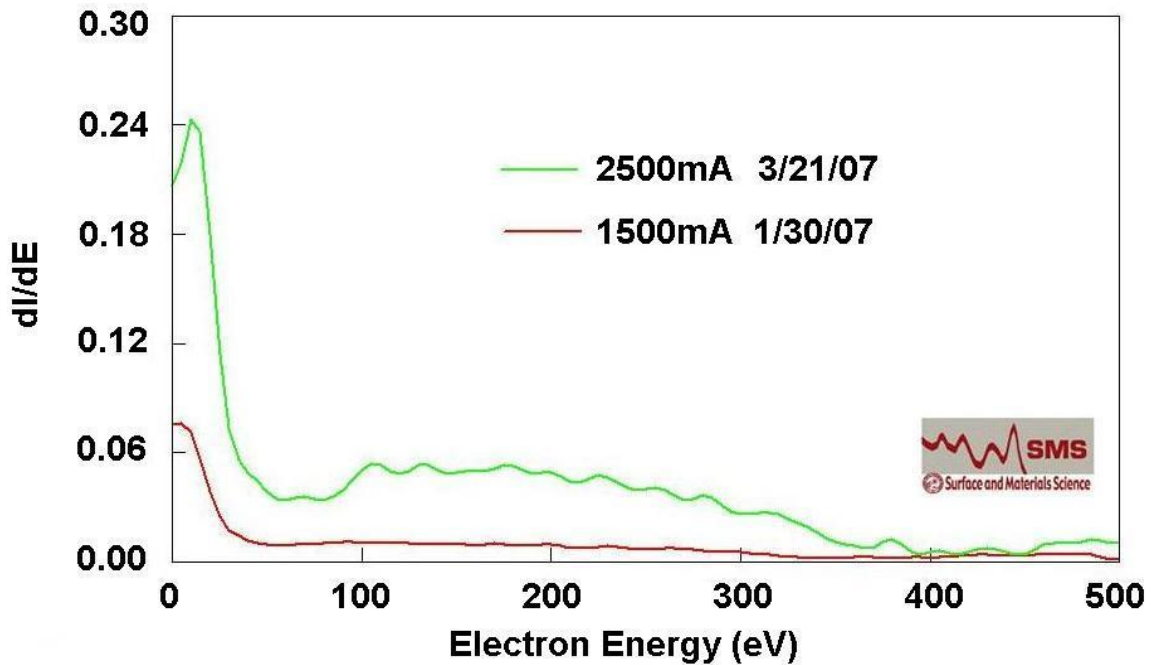


Figure 16. Electron energy distribution measured by the retarding field analyzer RFA at two different LER beam currents 1500 mA and 2500 mA. The energy spectrum is typically peaked at low energies ~2-10eV.

REFERENCES

- ¹ In Proceedings of the Workshops ELOUD07, ELOUD04, ELOUD02. See contributions K. Ohmi, M. Jimenez, G. Rumolo, K. Harkay, R. Macek, Kato, M. Furman, M. Palmer, Y. Suetsugu, F. Zimmerman *et al.* (2002).
- ² N. Phinney, N. Toge, N. Walker ILC-Report-2007-001 (2007).
- ³ M. T.F. Pivi *et al.* Appl. Phys. 104, 104904 (2008).
- ⁴ M. T.F. Pivi and J. Ng *et al.* *Observation of Magnetic Resonances in an Electron Cloud* Nucl. Instrum. Methods A, 621 (1-3), 33–38, (2010).
- ⁵ R. Rosenberg, K. Harkay Nucl. Instrum. Methods A453 (2000).
- ⁶ R. Macek *et al.* in Proceedings of the PAC03 Conference, ROAB003 (2003).
- ⁷ G. Arduini *et al.* in Proceedings of the EPAC00 Conference 259-261 (2000).
- ⁸ J.M. Jimenez, B. Henrist, J.M. Laurent, K. Weiss CERN-LHC-Project-Report-677, (2003).
- ⁹ R.E. Kirby, F. King. Nucl. Instrum. Methods A, A469, (2001).
- ¹⁰ F. Le Pimpec, R. Kirby, F. King *et al.* J. Vac. Sci. Tech. A23 (6), (2005).
- ¹¹ C. Scheuerlein, B. Henrist, N. Hilleret, C. Scheuerlein, M. Taborelli Appl. Surf. Sci., 172 : 95-102, (2001).
- ¹² R. Cimino, I. Collins *et al.* Phys. Rev. Lett. **93**, 014801, (2004).
- ¹³ M. Nishiwaki, S. Kato J. Vac. Sci. Tech. **A25**, 675, (2007).
- ¹⁴ Y. Suetsugu *et al.* Nucl. Instrum. Methods **A 554**, 92-113 (2005).
- ¹⁵ Y. Suetsugu, K. Kanazawa, K. Shibata, H. Hisamatsu, Nucl. Instrum. Methods **A 556**, 399-409 (2006).

-
- ¹⁶ F. Le Pimpec, R. Kirby, F. King and M. T.F. Pivi, Nucl. Instrum. Methods A 551 (2005) 187-199.
- ¹⁷ F. Le Pimpec, R. Kirby, F. King and M. T.F. Pivi, Nucl. Instrum. Methods A 564 (2006) 44–50.
- ¹⁸ P. He *et al.* in Proceedings of the EPAC 04 Conference (2004).
- ¹⁹ A. Fisher *LER Synchrotron-Light Power for the X-Ray Monitor*, SLAC-Note <http://www.slac.stanford.edu/~afisher/XRay/XrayPower/XrayPower.pdf>, April 2010.
- ²⁰ M. A. Furman and G. R. Lambertson, "*The Electron-Cloud Instability in the Arcs of the PEP-II Positron Ring*", LBNL-41123/CBP Note-246, (1997).
- ²¹ J. D. Jackson, *Classical Electrodynamics*, 2nd. ed. J. Wiley & Sons, (1975).
- ²² N. Hilleret *et al.*, in Proceedings of the EPAC00 Conference, THXF102 pp.217 (2000).
- ²³ F. Rieke and W. Prepejchal Phys. Rev. A6. 1507, (1972).
- ²⁴ B. Henrist, N. Hilleret, C. Scheuerlein, M. Taborelli, G. Vorlaufer *et al.*, Proceedings of the EPAC02 Conference, WEPDO014, Paris, France (2002).
- ²⁵ C. Benvenuti *et al.* in Proceedings of the EPAC98 Conference, 200-204 (1998).
- ²⁶ C. Benvenuti, P. Chiggiato, F. Cicoira, Y. L'Aminot, J. Vac. Sci. Technol. A 16(1), (1998), 148.
- ²⁷ V. Baglin, J. Bojko¹, O. Gröbner, B. Henrist, N. Hilleret, C. Scheuerlein, M. Taborelli in Proceedings of the EPAC Conference 211-217, Vienna, Austria (2000).
- ²⁸ S. De Santis *et al.* Physical Review Letters 100, 094801 (2008).
- ²⁹ M. Palmer *et al.* in Proceedings of the PAC09 Conference, FR1RAI02, Vancouver, Canada (2009).